JOURNAL OF MATERIALS SCIENCE **38** (2003) 2963–2970

Thermal stress distributions in axisymmetrically orthotropic fiber-reinforced composites with multilayered interfaces

L. H. YOU
College of Mechanical Engineering, Chongqing University, Chongqing City, 400044, People's Republic of China
E-mail: lyou@bournemouth.ac.uk

Treating fibrous composites with multilayered interfaces as a cylindrical assemblage consisting of multiple coaxial circular cylinders, a model has been developed with which the thermal stresses in such composites reinforced with axisymmetrically orthotropic fibers, can be analytically calculated. The developed model is employed to examine the influences of the volume fractions of the constituents as well as mechanical and physical properties of the interfacial layers on the thermal stresses in the composites. For the composites reinforced with different types of axisymmetrically orthotropic fibers, the effects of the volume fractions of the constituents on the stresses in the composites are different. The variety of mechanical and physical properties of the interfacial layers can greatly change the stress distributions in the composites. Therefore, reasonable design of the volume fractions of the constituents as well as mechanical and physical properties of the interfacial layers can help reduce the thermal stresses in the composites and improve the thermal mismatch of the composites under the thermal loading.

1. Introduction

Fibrous composites, due to their potentially superior properties at elevated temperatures, are viable candidates for developing a new generation of propulsion engines and structural components used in high-speed civil transport. However, because of different mechanical and physical properties of the constituents of fibrous composites, different deformations will occur in these constituents under a uniform temperature load, which result in different stresses. The stresses from this thermal mismatch may cause fiber breaks, debonds and cracks at interface, and plastic deformations of interfacial layers and matrix [1–3]. Plastic deformation may produce some potentially undesirable outcomes such as severely accelerated creep [2, 4], low cycle fatigue of one phase or the entire composite [5], dimensional instability [6, 7], or progressive sliding of one phase past the other [8]. It can also alter the initial yield surfaces and subsequent hardening response [9, 10]. Radial cracking at the fiber-matrix interface from circumferential thermal stresses during fabrication cool-down has been found in certain types of material systems such as silicon carbide-titanium aluminide composites [11]. Longitudinal and circumferential cracks at the fiber-matrix interface are also a source of concern [12].

Due to the above reasons, the research on thermal response of fibrous composites subjected to thermomechanical loading has become an active topic in composite mechanics, and some micromechanical models have been developed to understand the influence of the constituent properties on the evolution of thermal stresses. Roughly, there are three types of models: simple models, composite cylinder models and periodic fiber array models. The simple models utilized combinations of the Reuss and Voigt hypotheses for the state of stress and strain in the fiber and matrix phases. The periodic fiber array models, simplifying the circular cross section of the fibers as a rectangular cross section, modeled the fiber distribution in the matrix with a regular rectangular array of parallel fibers [9].

Among the three modeling approaches, composite cylinder models are most popular. Pagano and Tandon [13, 14] developed a model to approximate the elastic response of a composite body reinforced by coated fibers oriented in various directions. Using a four concentric cylinder model consisting of innermost transversely isotropic fiber, isotropic coating between the fiber and matrix, isotropic matrix, and outermost transversely isotropic composite, Mikata and Taya [15] obtained the elastic stress field in coated continuous fiber-reinforced composites under thermomechanical loading. Later, this model and two concentric cylinder model were employed to calculate the thermal residual stresses during the fabrication of Ni-coated carbon fiber composites [16]. These research studies treated the interfacial layer and matrix as fully elastic. In order to investigate the deformations and stresses when matrix becomes elastic-plastic, Zhang *et al*. [17] used

a two concentric cylinder model together with the increment theory of plasticity and obtained two partial differential equations governing the deformation behavior of composites. However, these two partial differential equations can only be solved numerically. In order to tackle this problem, Tresca's yield condition was introduced to develop the governing equation of a linear strain-hardening plastic coating [18] based on the four concentric cylinder model proposed by Mikata and Taya [15]. This approach was further extended to consider the effect of the linear strain-hardening elastic-plastic matrix on the deformations and stresses of the composite [19].

In the above composite cylinder models, only isotropic and transversely isotropic fibers were taken into account and the interfacial layer was treated as an isotropic or orthotropic coating. However, different types of axisymmetrically orthotropic fibers and multilayered interfaces have been reported. In the work of Avery and Herakovich [20], three types of axisymmetrically orthotropic fibers were discussed and their effects on the stresses in composites reinforced with such fibers were examined. Their work simplified the composites as a two concentric cylinder model and the interfacial layer was not considered. Multilayered interfaces normally arise in two situations: One is due to the chemical reaction at the fiber-matrix interface, the other is to introduce deliberately multiple coatings to improve the properties of the composites. DiCarlo [21], Wawner [22] and Lerch *et al*. [23] indicated that certain types of silicon carbide fibers used in SiC-Ti composites, such as the SCS6 fiber, consist of at least five concentric isotropic and orthotropic interfacial layers. Such composites with multilayered interfaces can be simplified as a multiple concentric cylinder model. By modifying the model of Mikata and Taya [15], Warwick and Clyne [24] proposed a system composed of a set of coaxial cylinders and applied it to SiC monofilament systems. Different types of axisymmetrically orthotropic fibers were not discussed and all the constituents of the composites were treated as fully elastic in their paper. Adopting the basic assumptions of Avery and Herakovich [20] and introducing the increment theory of plasticity, Pindera *et al*. [25] developed an iterative resolution method to determine the deformations and stresses in the composites. The matrix and interfacial layers of the composites have the property of a strain-hardening, elastic-plastic, von Mises solid and the core of the fibers is elastic and isotropic.

Using a different approach from that given in [20], in this paper, we will introduce a new analytical solution of deformations and stresses of continuous fiber-reinforced composites subjected to a uniform temperature change and employ it in the composites with multilayered interfaces. Although the plasticity of the interfacial layers and matrix has an obvious influence on the size of the deformations and stresses of the composites, our previous investigation indicates that the stress distribution in the composites with an elastic interfacial layer and matrix is similar in nature to that with an elastic-plastic interfacial layer and matrix [18]. Therefore, for the sake of simplicity, we can use a fully

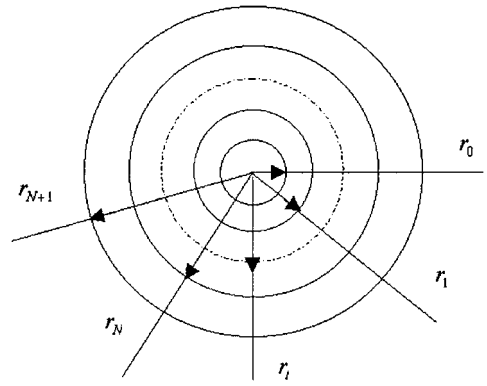

Figure 1 Composite model of multiple coaxial circular cylinders.

elastic model consisting of multiple concentric cylinders to investigate the thermal response of composites with axisymmetrically orthotropic fibers and multilayered interfaces. In the following, we firstly introduce such a model and its theory development.

2. Model and theory development

As shown in Fig. 1, the composites, consisting of an inner fiber, N middle interfacial layers, and an outer matrix subjected to a uniform temperature change, can be simplified as a concentric cylinder model where r_0 stands for the outer radius of the inner fiber, r_1 for the first interfacial layer, r_i for the ith interfacial layer, r_N for the last interfacial layer, and r_{N+1} for the outermost matrix.

Subject to a uniform temperature change, the deformations and stresses of the composites, consisting of an innermost axisymmetrically orthotropic fiber, middle multilayered interfaces and an outermost isotropic matrix, are axisymmetric. Without considering shear stresses, and denoting the radial displacement with u, the strain-displacement relationship can be written as

$$\begin{aligned} \varepsilon_r &= \frac{\mathrm{d}u}{\mathrm{d}r} \\ \varepsilon_\theta &= \frac{u}{r} \end{aligned} \tag{1}$$

Using $c_{ij}(i,\ j = \theta, r, z)$ to represent the stiffness coefficients, the elastic stress-strain relation for the axisymmetrically orthotropic fiber and interfacial layers has the form of

$$\begin{aligned} \sigma_r &= \sum_{j=r,\theta,z} c_{rj}(\varepsilon_j - \alpha_j \Delta T) \\ \sigma_\theta &= \sum_{j=r,\theta,z} c_{\theta j}(\varepsilon_j - \alpha_j \Delta T) \\ \sigma_z &= \sum_{j=r,\theta,z} c_{zj}(\varepsilon_j - \alpha_j \Delta T) \end{aligned} \tag{2}$$

where α_r, α_θ and α_z are the thermal expansion coefficients of the fiber and interfacial layers along radial, circumferential and axial directions, respectively, and ΔT is the temperature change.

For the isotropic elastic matrix, the stiffness coefficients of the composites in the above equations can

be determined with two constants: Young's modulus E and Poisson's ratio ν.

According to the theory of axisymmetric problems, the stress equilibrium of the composites can be described with the following equations

$$\frac{\mathrm{d}\sigma_r}{\mathrm{d}r} + \frac{\sigma_r - \sigma_\theta}{r} = 0 \qquad \frac{\mathrm{d}\sigma_z}{\mathrm{d}z} = 0 \tag{3}$$

The second of Equation 3 gives a constant axial stress. For the ith constituent, this constant stress is assumed to be a_i. Substituting it into the third of Equation 2 and solving for the axial strain ε_z, the relation among the axial strain ε_z and the radial and circumferential strains is determined. Then substituting ε_z into the first two of Equation 2, making use of Equation 1 to remove radial and circumferential strains, and substituting the radial and circumferential stresses into the first of Equation 3, we obtain an ordinary differential equation whose resolution gives the following radial displacement u

$$u_i = a_i D_i r + b_i r^{\lambda_{i1}} + c_i r^{\lambda_{i2}} + F_i r \tag{4}$$

where

$$\begin{aligned}
\lambda_{i1,i2} &= \pm\sqrt{\frac{c_{zzi}c_{\theta\theta i} - c_{z\theta i}c_{\theta zi}}{c_{zzi}c_{rri} - c_{zri}c_{rzi}}} \\
D_i &= \frac{c_{rzi} - c_{\theta zi}}{G_i} \\
F_i &= \frac{(H_i\alpha_{\theta i} + L_i\alpha_{ri})\Delta T}{G_i} \\
G_i &= c_{zzi}c_{\theta\theta i} + c_{zri}c_{rzi} - c_{zzi}c_{rri} - c_{z\theta i}c_{\theta zi} \\
H_i &= c_{zzi}c_{\theta\theta i} + c_{z\theta i}c_{rzi} - c_{zzi}c_{r\theta i} - c_{z\theta i}c_{\theta zi} \\
L_i &= c_{zzi}c_{\theta ri} + c_{zri}c_{rzi} - c_{zzi}c_{rri} - c_{\theta zi}c_{zri}
\end{aligned} \tag{5}$$

and a_i, b_i and c_i are the unknown constants, the subscript $i = 0$ stands for the fiber, and $i = 1, 2, \ldots, N$ for the ith interfacial layer.

The radial and circumferential strains can be determined from Equation 1 according to the known radial displacement u. The axial strain can be determined as follows by substituting the radial and circumferential strains into the third of Equation 2

$$\varepsilon_{zi} = A_{i1}a_i + A_{i2}b_i r^{\lambda_{i1}-1} + A_{i3}c_i r^{\lambda_{i2}-1} + A_{i4} \tag{6}$$

where

$$\begin{aligned}
A_{i1} &= \frac{1 - D_i(c_{z\theta i} + c_{zri})}{c_{zzi}} \\
A_{i2} &= -\frac{c_{z\theta i} + \lambda_{i1}c_{zri}}{c_{zzi}} \\
A_{i3} &= -\frac{c_{z\theta i} + \lambda_{i2}c_{zri}}{c_{zzi}} \\
A_{i4} &= \frac{1}{c_{zzi}}(c_{z\theta i}\alpha_{\theta i} + c_{zri}\alpha_{ri} + c_{zzi}\alpha_{zi})\Delta T \\
&\quad - \frac{F_i(c_{z\theta i} + c_{zri})}{c_{zzi}}
\end{aligned} \tag{7}$$

All the stresses can be obtained by substituting the radial, circumferential and axial strains into Equation 2 which can be written as

$$\begin{aligned}
\sigma_{ri} &= A_{i5}a_i + A_{i6}b_i r^{\lambda_{i1}-1} + A_{i7}c_i r^{\lambda_{i2}-1} + A_{i8} \\
\sigma_{\theta i} &= A_{i9}a_i + A_{i10}b_i r^{\lambda_{i1}-1} + A_{i11}c_i r^{\lambda_{i2}-1} + A_{i12} \\
\sigma_{zi} &= a_i
\end{aligned} \tag{8}$$

where

$$\begin{aligned}
A_{i5} &= \frac{c_{rzi}}{c_{zzi}} + D_i\left[c_{r\theta i} + c_{rri} - \frac{c_{rzi}}{c_{zzi}}(c_{z\theta i} + c_{zri})\right] \\
A_{i6} &= c_{r\theta i} + \lambda_{i1}c_{rri} - \frac{c_{rzi}}{c_{zzi}}(c_{z\theta i} + \lambda_{i1}c_{zri}) \\
A_{i7} &= c_{r\theta i} + \lambda_{i2}c_{rri} - \frac{c_{rzi}}{c_{zzi}}(c_{z\theta i} + \lambda_{i2}c_{zri}) \\
A_{i8} &= F_i\left[c_{r\theta i} + c_{rri} - \frac{c_{rzi}}{c_{zzi}}(c_{z\theta i} + c_{zri})\right] \\
&\quad + \left[\frac{c_{rzi}}{c_{zzi}}(c_{z\theta i}\alpha_{\theta i} + c_{zri}\alpha_{ri}) \right. \\
&\quad \left. - (c_{r\theta i}\alpha_{\theta i} + c_{rri}\alpha_{ri})\right]\Delta T \\
A_{i9} &= \frac{c_{\theta zi}}{c_{zzi}} + D_i\left[c_{\theta\theta i} + c_{\theta ri} - \frac{c_{z\theta i}}{c_{zzi}}(c_{\theta zi} + c_{zri})\right] \\
A_{i10} &= c_{\theta\theta i} + \lambda_{i1}c_{\theta ri} - \frac{c_{z\theta i}}{c_{zzi}}(c_{\theta zi} + \lambda_{i1}c_{zri}) \\
A_{i11} &= \left[c_{\theta\theta i} + \lambda_{i2}c_{\theta ri} - \frac{c_{z\theta i}}{c_{zzi}}(c_{\theta zi} + \lambda_{i2}c_{zri})\right. \\
A_{i12} &= F_i\left[c_{\theta\theta i} + c_{\theta ri} - \frac{c_{z\theta i}}{c_{zzi}}(c_{\theta zi} + c_{zri})\right] \\
&\quad + \left[\frac{c_{\theta zi}}{c_{zzi}}(c_{z\theta i}\alpha_{\theta i} + c_{zri}\alpha_{ri}) \right. \\
&\quad \left. - (c_{\theta\theta i}\alpha_{\theta i} + c_{\theta ri}\alpha_{ri})\right]\Delta T
\end{aligned} \tag{9}$$

Similarly, with the Young's modulus E_m and Poisson's ratio v_m where the subscript m represents the matrix, we can determine the concrete forms of stiffness coefficients of the matrix. Then following the above treatment, the radial displacement, and strain and stress components of the matrix can be obtained. Some of them are given below.

$$u_{N+1} = b_{N+1}r + c_{N+1}r^{-1} \tag{10}$$

$$\begin{aligned}
\varepsilon_{zN+1} &= \frac{1 - v_m - 2v_m^2}{(1 - v_m)E_m}a_{N+1} \\
&\quad - \frac{2v_m}{1 - v_m}b_{N+1} + \frac{1 + v_m}{1 - v_m}\alpha_m\Delta T
\end{aligned} \tag{11}$$

$$\sigma_{rN+1} = \frac{v_m}{1-v_m}a_{N+1} + \frac{E_m}{1-v_m}b_{N+1} - \frac{E_m}{1+v_m}c_{N+1}r^{-2} - \frac{E_m}{1-v_m}\alpha_m \Delta T$$

$$\sigma_{\theta N+1} = \frac{v_m}{1-v_m}a_{N+1} + \frac{E_m}{1-v_m}b_{N+1} + \frac{E_m}{1+v_m}c_{N+1}r^{-2} - \frac{E_m}{1-v_m}\alpha_m \Delta T \quad (12)$$

$$\sigma_{zN+1} = a_{N+1}$$

For the composites consisting of an inner fiber, N middle interfacial layers, and an outer matrix, there are $3(N+2)$ unknown constants in Equations 4, 6, 8, 10, 11 and 12. The conditions determining these unknown constants are:

1. at the center of the cross section of fibers, the radial displacement cannot be an infinitely big value, i.e.,

$$u_0 \text{ is a bounded value} \quad \text{at } r = 0 \quad (13)$$

2. at the interface between the ith interfacial layer and $(i+1)$th interfacial layer including the innermost fiber and outermost matrix, the radial displacement, axial strain and radial stress should have the same values, i.e.,

$$u_i = u_{i+1}, \varepsilon_{zi} = \varepsilon_{zi+1}, \sigma_{ri} = \sigma_{ri+1} \quad \text{at } r = r_i \quad (i = 0, 1, 2, \ldots, N) \quad (14)$$

3. at the outer radius of the outermost matrix, the radial stress is zero, i.e.

$$\sigma_{rN+1} = 0 \quad \text{at } r = r_{N+1} \quad (15)$$

4. along the axial direction of the fiber, there is no externally applied axial force, i.e.,

$$\int_0^{r_0} \sigma_{z0} r \mathrm{d}r + \sum_{i=0}^{N-1} \int_{r_i}^{r_{i+1}} \sigma_{zi+1} r \mathrm{d}r + \int_{r_N}^{r_{N+1}} \sigma_{zN+1} r \mathrm{d}r = 0 \quad (16)$$

Substituting the radial displacements, axial strains, radial stresses and axial stresses of the fiber, interfacial layers and matrix into the above Equations 13 to 16, we obtain $3(N+2)$ linear algebra equations whose resolution determines $3(N+2)$ unknown constants a_i, b_i and $c_i (i = 0, 1, 2, \ldots, N+1)$. The substitution of these unknown constants into Equations 4, 8, 10 and 12 gives the radial displacement, and radial, circumferential and axial stresses.

3. Numerical applications

With the above-developed method, in this section, we investigate the stresses in composites consisting of an axisymmetrically orthotropic fiber, 4 interfacial layers and a matrix. Three types of axisymmetrically orthotropic fibers were considered. For the first type of fibers (FTF), the Young's moduli and thermal expansion coefficients in the circumferential and axial directions are the same. For the second type of fibers (STF), these material properties in the radial and axial directions are the same. For the third type of fibers (TTF), the material properties in radial and circumferential directions are the same. The outermost matrix was treated as isotropic. The mechanical and physical properties of the fiber and matrix were given in Table I where NOM represents the number of the constituent materials. The innermost three interfacial layers were also taken to be axisymmetrically orthotropic and the outermost interfacial layer was taken to be isotropic. Their mechanical and physical properties were given in Table II where NOIL stands for the number of the interfacial layers. The externally applied load is a uniform temperature increase $\Delta T = 500^\circ$C.

The effect of the different volume fractions of the constituents on the thermal stresses in the composites is first examined. For doing this, three cases of different volume fractions were taken into account. The corresponding outer radii of the fiber, interfacial layers and matrix were listed in Table III, and their volume fractions were given in the parentheses of the table. It can be seen that the interfacial layers have the same volume fractions for Case I and Case II. However, the volume fraction of the fiber was increased and the volume fraction of the matrix was decreased from Case I to Case II.

TABLE I Mechanical and physical properties of fiber and matrix

NOM	E_z (GPa)	E_θ (GPa)	E_r (GPa)	$v_{z\theta}$	v_{zr}	$v_{\theta r}$	α_z ($10^{-6}/^\circ$C)	α_θ ($10^{-6}/^\circ$C)	α_r ($10^{-6}/^\circ$C)
FTF	220	220	27.5	0.2	0.25	0.25	0.28	0.28	5.56
STF	220	27.5	220	0.2	0.25	0.025	0.28	5.56	0.28
TTF	220	27.5	27.5	0.2	0.2	0.25	0.28	5.56	5.56
Matrix	34.5	34.5	34.5	0.12	0.12	0.12	1.11	1.11	1.11

TABLE II Mechanical and physical properties of interfacial layers

NOIL	E_z (GPa)	E_θ (GPa)	E_r (GPa)	$v_{z\theta}$	v_{zr}	$v_{\theta r}$	α_z ($10^{-6}/^\circ$C)	α_θ ($10^{-6}/^\circ$C)	α_r ($10^{-6}/^\circ$C)
1st	170	7	170	0.08	0.19	0.04	1.8	28	1.8
2nd	410	410	180	0.2	0.25	0.25	2.5	2.5	6
3rd	310	60	60	0.15	0.15	0.2	1.5	7.5	7.5
4th	80	80	80	0.3	0.3	0.3	8	8	8

TABLE III Outer radii and volume fractions of the constituents of composites

Case	r_0 (μm)	r_1 (μm)	r_2 (μm)	r_3 (μm)	r_4 (μm)	r_5 (μm)
I	20 (0.16)	23 (0.0516)	26 (0.0588)	29 (0.066)	32 (0.0732)	50 (0.5904)
II	26 (0.2704)	28.37 (0.0516)	30.85 (0.0588)	33.42 (0.066)	36.05 (0.0732)	50 (0.4802)
III	26 (0.2704)	30.56 (0.1032)	35.04 (0.1176)	39.47 (0.132)	43.86 (0.1464)	50 (0.2305)

For Case II and Case III, the volume fraction of the fiber was kept unchanged, but the volume fractions of the interfacial layers were doubled and the volume fraction of the matrix was further reduced.

For the composite reinforced with the first type of fibers (FTF), the obtained circumferential and axial stresses were given in Figs 2a and b, respectively where, I, II and III stand for Case I, Case II and Case III in Table III respectively, and FTF indicates that the composite is reinforced with the first type of axisymmetrically orthotropic fibers. Since the radial stress is very small compared to the circumferential and axial stresses, it is not given here for saving space. Clearly, different volume fractions result in different circumferential and axial stresses. Increasing the volume fraction of the fiber and keeping the volume fractions of the interfacial layers unchanged, the maximum circumferential and axial stresses in the fiber decrease, but those (their absolute values) in the interfacial layers increase slightly. Oppositely, raising the volume fractions of the interfacial layers increases the maximum circumferential and axial stresses in the fiber, but reduces those in the interfacial layers. Due to the highest axial Young's modulus of the 2nd interfacial layer among all the interfacial layers and lower axial thermal expansion coefficients of its neighboring interfacial layers, the absolute value of its axial stress is larger than those of its neighboring interfacial layers. Due to the very big differences of the axial Young's moduli and axial thermal expansion coefficients between the 3rd and 4th interfacial layers, a very big jump of axial stresses occurs between these two interfacial layers. In contrast, the differences of circumferential Young's moduli and circumferential thermal expansion coefficients between these two interfacial layers are small. Consequently, a small jump of the circumferential stresses occurs between these two interfacial layers. Because of the big differences of the thermal expansion coefficient and Young's modulus between the 4th interfacial layer and matrix, very big jumps of the axial and circumferential stresses occur between them.

For the composite reinforced with the second type of fibers (STF), the calculated radial, circumferential and axial stresses were depicted in Fig. 3a, b and c, respectively where STF means that the composite is reinforced with the second type of axisymmetrically orthotropic fibers. Same as above, the volume fractions have an obvious effect on the stresses in the composite. When the volume fraction of the fiber is increased,

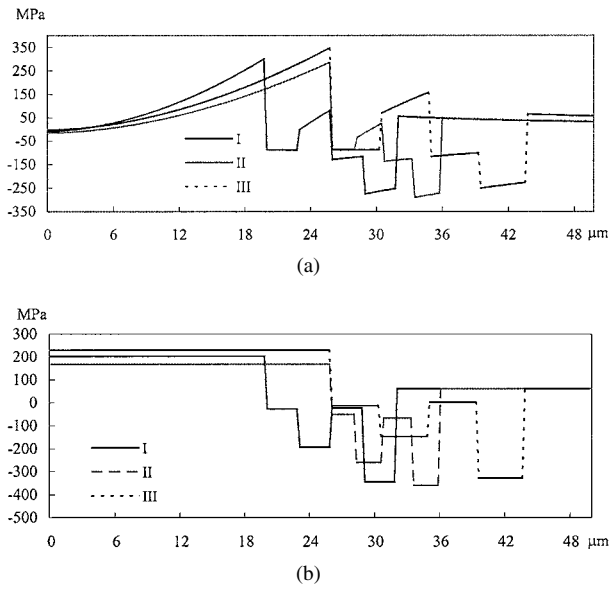

Figure 2 (a) Circumferential stresses in composites with FTF (The properties of the interfacial layers are from Table 2) and (b) Axial stresses in composites with FTF (The properties of the interfacial layers are from Table 2).

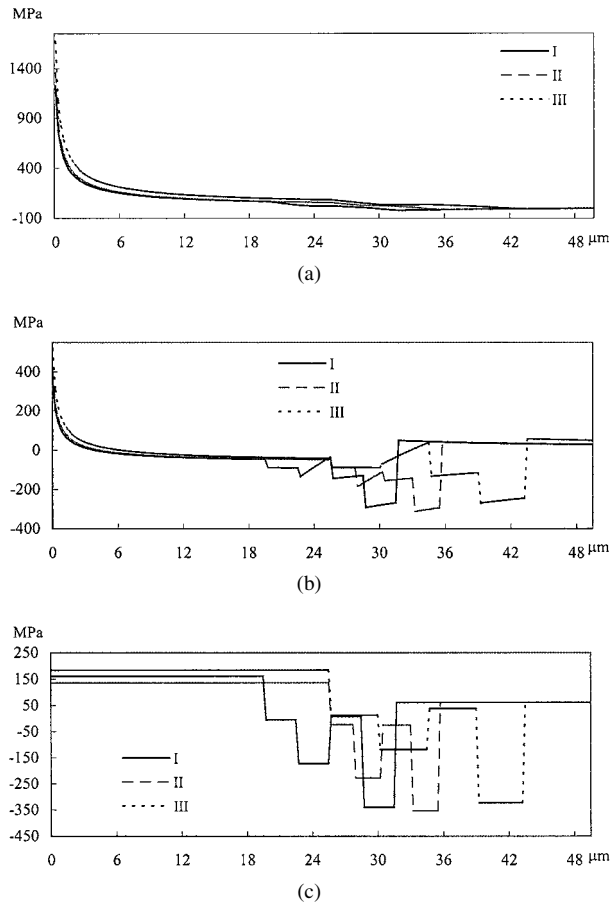

Figure 3 (a) Radial stresses in composites with STF (The properties of the interfacial layers are from Table 2), (b) Circumferential stresses in composites with STF (The properties of the interfacial layers are from Table 2) and (c) Axial stresses in composities with STF (The properties of the interfacial layers are from Table 2).

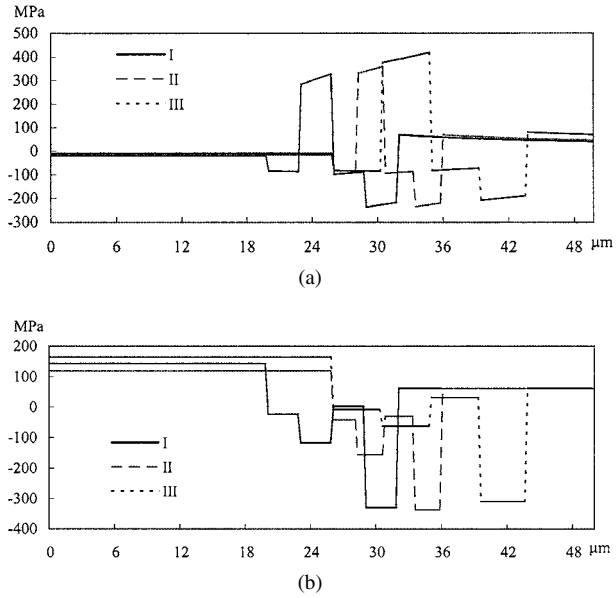

Figure 4 (a) Circumferential stresses in composites with TTF (The properties of the interfacial layers are from Table 2) and (b) Axial stresses in composites with TTF (The properties of the interfacial layers are from Table 2).

the axial stress in the fiber is decreased, but the maximum radial and circumferential stresses in the fiber are obviously increased. The maximum circumferential and axial stresses in the interfacial layers also have a small increase. When the volume fractions of the interfacial layers go up, all the stresses in the fiber rise noticeably, but the maximum circumferential and axial stresses in the interfacial layers drop. Unlike the composite reinforced with the first type of axisymmetrically orthotropic fibers, the maximum radial stress in the fiber for the composite reinforced with the second type of axisymmetrically orthotropic fibers is the largest among all the stresses in the composite. Therefore, for the composite reinforced with the second type of axisymmetrically orthotropic fibers, small volume fractions of the interfacial layers and thin fibers can effectively lower the maximum radial stress in the fiber and improve the loading capacity of the composite.

For the composite reinforced with the third type of fibers (TTF), the obtained circumferential and axial stresses were shown in Fig. 4a and b where TTF denotes that the composite is reinforced with the third type of axisymmetrically orthotropic fibers. Due to the same reason, the radial stress in not provided here. Raising the volume fraction of the fiber reduces the axial stress, affects little the circumferential stress in the fiber. In addition, it slightly increases the maximum circumferential and axial stresses in the interfacial layers. Except for obvious influences on the axial stress in the fiber, the volume fractions of the interfacial layers have a very small effect on the circumferential stress in the fiber. Doubling the volume fractions of the interfacial layers, the axial stress in the fiber and the maximum circumferential stress in the interfacial layers increase, but the maximum axial stress in the interfacial layers decreases. Since the circumferential thermal expansion coefficients of the 1st and 3rd interfacial layers are far higher than that of the 2nd interfacial layer, larger circumferential thermal deformations occur in the 1st and 3rd interfacial layers which pull the 2nd interfacial layer along the circumferential direction leading to the very large tensile circumferential stresses in the 2nd interfacial layer. The high axial stress in the 4th interfacial layer is mainly due to the big differences of Young's moduli and thermal expansion coefficients between the 4th interfacial layer and the matrix.

Due to the very low Young's modulus of the matrix, the varieties of the volume fractions of the constituents basically have no influences on all the stresses in the matrix for the composites reinforced with the three types of axisymmetrically orthotropic fibers. For all the composites discussed above, all the stresses in the interfacial layers differ from each other greatly because of the different mechanical and physical properties of these interfacial layers.

The differences of mechanical and physical properties between the fiber, interfacial layers and matrix given by Tables I and II are noticeable. As a result, high thermal mismatch stresses appear in the composites. In the following, we will indicate how different mechanical and physical properties of the interfacial layers affect the stress distributions of the composites. For doing this, we made four changes for the mechanical and physical properties of interfacial layers given in Table II. Firstly, the thermal expansion coefficients in the interfacial layers adjacent to the fiber and matrix were taken to be close to those of the fiber and matrix. Secondly, axial and radial Young's moduli of the 1st interfacial layer were greatly decreased to make it deform more easily. Thirdly, the differences of Young's moduli between the 4th interfacial layer and matrix were dropped. Fourthly, the large Young's moduli in the 2nd and 3rd interfacial layers were lowered to reduce the differences of Young's moduli between the interfacial layers. The modified mechanical and physical properties of the interfacial layers were given in Table IV. The obtained stresses were depicted in Figs 5 to 7 for the composites reinforced with the first, second and third types of axisymmetrically orthotropic fibers, respectively. Same as above, the radial stress in the composites reinforced with the first and third types of axisymmetrically orthotropic fiber, respectively, is very small compared with the circumferential and axial stresses; it is not given here.

TABLE IV Modified mechanical and physical properties of interfacial layers

NOIL	E_z (GPa)	E_θ (GPa)	E_r (GPa)	$v_{z\theta}$	v_{zr}	$v_{\theta r}$	α_z (10^{-6}/°C)	α_θ (10^{-6}/°C)	α_r (10^{-6}/°C)
1st	70	7	70	0.08	0.19	0.04	1.8	6	1.8
2nd	130	130	100	0.2	0.25	0.25	2.5	2.5	6
3rd	120	60	60	0.15	0.15	0.2	1.5	7.5	7.5
4th	50	50	50	0.3	0.3	0.3	2	2	2

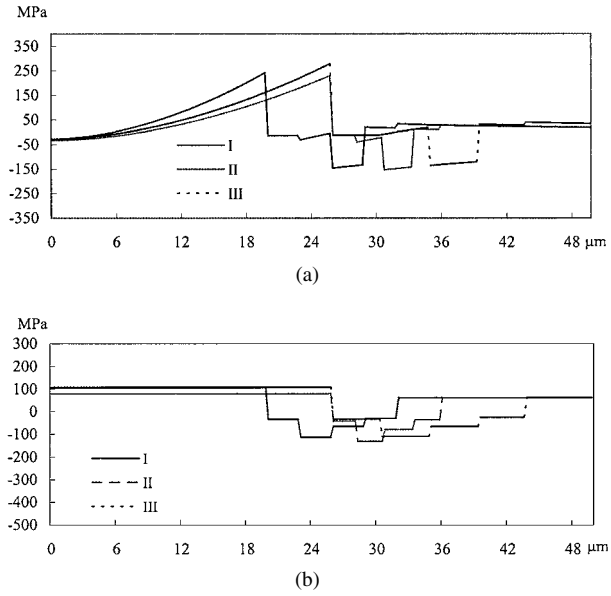

Figure 5 (a) Circumferential stresses in composites with FTF (The properties of the interfacial layers are from Table 4) and (b) Axial stresses in composites with FTF (The properties of the interfacial layers are from Table 4).

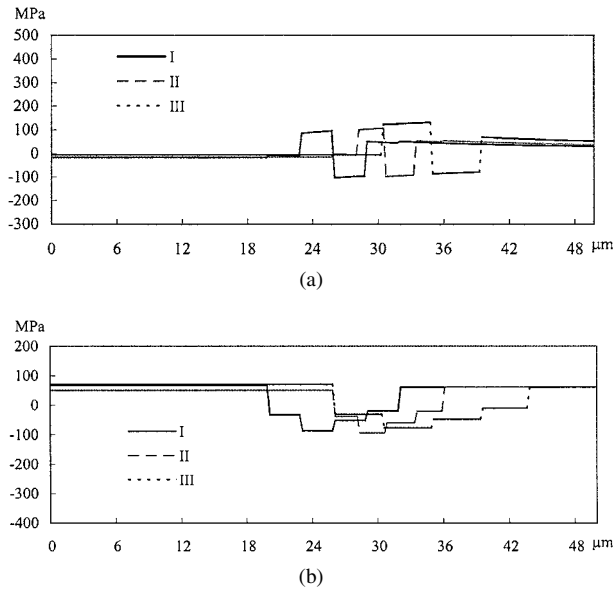

Figure 7 (a) Circumferential stresses in composites with TTF (The properties of the interfacial layers are from Table 4) and (b) Axial stresses in composites with TTF (The properties of the interfacial layers are from Table 4).

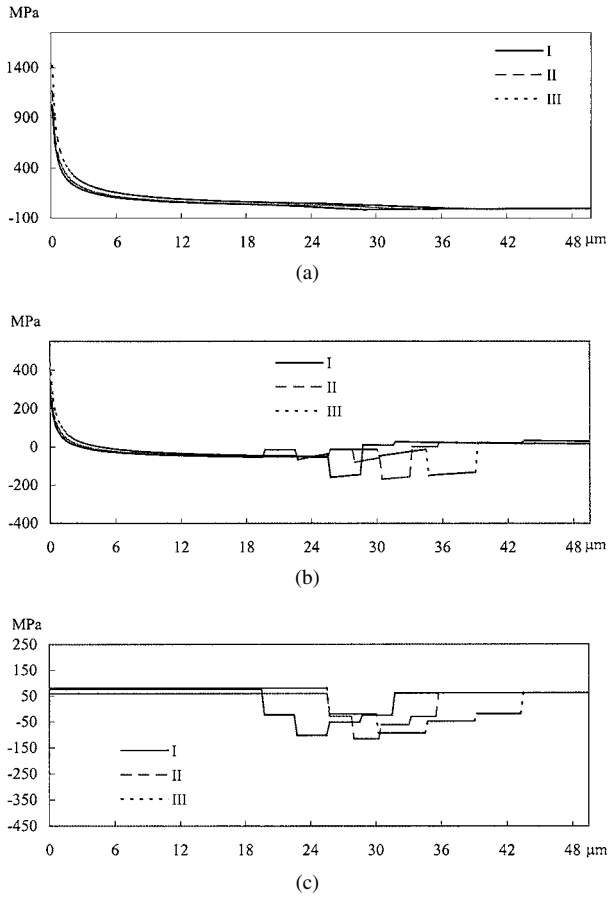

Figure 6 (a) Radial stresses in composites with STF (The properties of the interfacial layers are from Table 4), (b) Circumferential stresses in composites with STF (The properties of the interfacial layers are from Table 4) and (c) Axial stresses in composites with STF (The properties of the interfacial layers are from Table 4).

Comparing Fig. 2 with 5, 3 with 6, and 4 with 7, three conclusions can be drawn. Firstly, the maximum stresses in the fiber for the three types of the composites have been obviously decreased after using the modified mechanical and physical properties. The reasons for this are obvious. The circumferential thermal expansion coefficient of the 1st interfacial layer was reduced from $28 \times 10^{-6}/^{\circ}\mathrm{C}$ to $6 \times 10^{-6}/^{\circ}\mathrm{C}$ which is closer to that of the fiber. The small discrepancy of the thermal expansion coefficients between the fiber and the 1st interfacial layer caused small deformation differences. Moreover, the axial and radial Young's moduli of the 1st interfacial layer were decreased from 170 GPa to 70 GPa. They applied a smaller restraint force to the fiber leading to smaller stresses in the fiber. Secondly, the differences of the circumferential and axial stresses between the 4th interfacial layer and matrix become much smaller after the application of the modified mechanical and physical properties of the interfacial layers. The decrease of the thermal expansion coefficients of the 4th interfacial layer from $8 \times 10^{-6}/^{\circ}\mathrm{C}$ to $2 \times 10^{-6}/^{\circ}\mathrm{C}$ lowers the thermal deformation discrepancy between the 4th interfacial layer and matrix, and Young's modulus of the 4th interfacial layer approaching that of the matrix makes them have a closer deformation resistance resulting in the small stress differences. Finally, the stress variety between different interfacial layers was reduced greatly and the maximum stresses in the interfacial layers were lowered dramatically since the discrepancies of Young's moduli between the interfacial layers become much smaller and the maximum difference of the thermal expansion coefficients between them is noticeably decreased.

It should be pointed out that the influences of mechanical and physical properties of the interfacial layers on the stresses in the composites are complicated. How to properly combine them with those of the fiber and matrix is an important issue for the design of such composites. Optimization techniques can be employed to obtain a more reasonable design of the mechanical and physical properties of interfacial layers, fiber and matrix for reducing the thermal mismatch of different constituents and improving the stress distributions in the composites.

4. Conclusions

In this paper, we have presented a micromechanics model to carry thermal analysis of composites reinforced with axisymmetrically orthotropic fibers. Multilayered interfaces can be analytically dealt with using the proposed model.

Applying the developed model, we examined how different volume fractions of the constituents affect the thermal stresses in the composites. For the composites reinforced with different types of axisymmetrically orthotropic fibers, the effects of different volume fractions of the constituents on the stresses in the composites are different. For the composite reinforced with the first type of axisymmetrically orthotropic fibers, large volume fraction of the fiber and low volume fractions of the interfacial layers can reduce the maximum circumferential and axial stresses in the fiber. However, they will increase circumferential and axial stresses in the interfacial layers. For the composite reinforced with the second type of axisymmetrically orthotropic fibers, the radial stress in the fiber is the largest among all the stresses in the composite. Small volume fractions of the fiber and interfacial layers can greatly lower the maximum value of the radial stress. For the composite reinforced with the third type of axisymmetrically orthotropic fibers, small volume fraction of the fiber can raise the axial stress in the fiber, but reduced the circumferential and axial stresses in the interfacial layers. Increasing the volume fractions of the interfacial layers, the axial stresses in the fiber and the maximum circumferential stress in the interfacial layers will increase, but the maximum axial stress in the interfacial layers will decrease.

We have also discussed how mechanical and physical properties of the interfacial layers affect the stress distributions in the composites reinforced with different types of axisymmetrically orthotropic fibers. It is found that different mechanical and physical properties of interfacial layers can greatly change the stresses in the composites. In order to reduce the stresses in the fiber and interfacial layers, and the stress differences between the constituents, the interfacial layers with low Young's moduli should be employed and the thermal expansion coefficients of the interfacial layers adjacent to the fiber and matrix should not be far higher or lower than those of the fiber and matrix, respectively.

References

1. M. Y. WU, J. WADSWORTH and O. D. SHERBY, *Metall. Trans. A, Phys. Metall. and Mater. Sci*. **18A** (1987) 451.
2. G. S. DAEHN and G. GONZALEZ-DONCEL, *ibid.* **20A** (1989) 2355.
3. S. M. PICKARD and B. DERBY, *Acta. Metall. et Mater*. **38** (1990) 2537.
4. H. ZHANG, G. S. DAEHN and R. H. WAGONER, *Scripta Metall. et Mater*. **24** (1990) 2151.
5. G. GARMONG, *Metall. Trans*. **5** (1974) 2199.
6. M. A. WRIGHT, *Metall. Trans. A, Phys. Metall. and Mater. Sci*. **6A** (1975) 129.
7. S. YODA, N. KURIHARA, K. WAKASHIMA and S. UMEKAWA, *ibid.* **9A** (1978) 1229.
8. S. YODA, K. TAKAHASHI, K. WAKASHIMA and S. UMEKAWA, *ibid.* **10A** (1979) 1796.
9. J. ABOUDI, *Int. J. Eng. Sci*. **23** (1985) 773.
10. T. FUJITA, M. J. PINDERA and C. T. HERAKOVICH, in "Thermal and Mechanical Behavior of Metal Matrix and Ceramic Matrix Composites, ASTM STP 1080," edited by J. M. Kennedy, H. H. Moeller and W. S. Johnson (American Society for Testing and Materials, Philadelphia, PA, 1990) p. 165.
11. P. K. BRINDLEY, R. A. MACKAY and P. A. BARTOLOTTA, NASA Technical Memorandum 103279, Lewis Research Center, 1990.
12. W. S. JOHNSON, S. J. LUBOWINSKI and A. L. HIGHSMITH, in "ASTM STP 1080," edited by J. M. Kennedy, H. H. Moeller and W. S. Johnson (American Society for Testing and Materials, Philadelphia, PA, 1990) p. 193.
13. N. J. PAGANO and G. P. TANDON, *Comp. Sci. and Tech*. **31** (1988) 273.
14. *Idem., ibid*. **38** (1990) 247.
15. Y. MIKATA and M. TAYA, *J. Comp. Mater*. **19** (1985) 554.
16. Y. MIKATA, T. TAKAHASHI, S. K. SU and Y. UCHIDA, *Bull. Chem. Soc. Jpn*. **60** (1987) 2593.
17. H. ZHANG, P. M. ANDERSON and G. S. DAEHN, *Metall. and Mater. Trans. A* **25A** (1994) 415.
18. L. H. YOU and S. LONG, *Composites* Part A **29A** (1998) 1185.
19. L. H. YOU, S. LONG and L. ROHR, *J. Appl. Mech., Trans. Amer. Soc. Mech. Eng*. **66** (1999) 750.
20. W. B. AVERY and C. T. HERAKOVICH, *ibid.* **53** (1986) 751.
21. J. A. DICARLO, in "International Conference on Whisker- and Fiber-Toughened Ceramics," edited by R. A. Bradley, D. E. Clark, D. S. Larsen and J. Q. Stiegler (USA, ASM International Metals Park, OH, 1988) p. 1.
22. F. E. WAWNER, in "Fibre Reinforcements for Composite Materials," edited by A. R. Bunsell (Amsterdam, Elsevier, The Netherlands, 1988) p. 371.
23. B. A. LERCH, D. R. HULL and T. A. LEONHARDT, NASA Technical Memorandum 100938, Lewis Research Center, 1988.
24. C. M. WARWICK and T. W. CLYNE, *J. Mater. Sci.* **26** (1991) 3817.
25. M. J. PINDERA, A. D. FREED and S. M. ARNOLD, *Int. J. Solids and Struc.* **30** (1993) 1213.

Received 28 March 2002
and accepted 18 April 2003